Dual-mode mechanical resonance of individual ZnO nanobelts

X. D. Bai,[a] P. X. Gao, and Z. L. Wang[b]
School of Materials Science and Engineering, Georgia Institute of Technology, Atlanta, Georgia 30332-0245

E. G. Wang
International Center for Quantum Structures and State Key Laboratory for Surface Physics, Institute of Physics, Chinese Academy of Sciences, Beijing 100080, China

(Received 7 March 2003; accepted 29 April 2003)

The mechanical resonance of a single ZnO nanobelt, induced by an alternative electric field, was studied by *in situ* transmission electron microscopy. Due to the rectangular cross section of the nanobelt, two fundamental resonance modes have been observed corresponding to two orthogonal transverse vibration directions, showing the versatile applications of nanobelts as nanocantilevers and nanoresonators. The bending modulus of the ZnO nanobelts was measured to be ~ 52 GPa and the damping time constant of the resonance in a vacuum of 5×10^{-8} Torr was ~ 1.2 ms and quality factor $Q=500$. © *2003 American Institute of Physics.* [DOI: 10.1063/1.1587878]

Cantilever-based sensors present a wide range applications in the field of physical, chemical, and biochemical sciences.[1–3] Miniaturization of the cantilever dimensions toward the nanometer scale will enable an improvement in sensitivity, spatial resolution, energy efficiency, and time of response.[4,5] Recently, ultralong, beltlike, quasi-one-dimensional nanostructures (so called nanobelts or nanoribbons) have been synthesized for semiconducting oxides of zinc, tin, indium, cadmium, and gallium, by simply evaporating the desired commercial metal–oxide powders at high temperatures.[6] The as-synthesized oxide nanobelts are pure, structurally uniform, single crystalline, and most of them are free from dislocations. The beltlike morphology appears to be a unique and common structural characteristic for the family of semiconducting oxides with cations of different valence states and materials of distinct crystallographic structures. The nanobelts are an ideal system for fully understanding dimensionally confined transport phenomena in functional oxides and building functional devices along individual nanobelts.

Semiconducting oxide nanobelts[6] and nanowires[7] have shown electronic, chemical, and optical properties.[8,9] Nanowires are the fundamental building blocks for fabricating nanoscale sensors and logic circuits.[10,11] The nanobelts have a distinct structural morphology, characterized by a rectangular cross section and a uniform structure, which could be directly used as nanocantilevers and nanoresonators in nanoelectromechanical systems (NEMS).[12,13] A key phenomenon for applying nanobelts in NEMS technology is their mechanical resonance behavior, and an important physical quantity for cantilever applications is their bending modulus. In this letter, the mechanical resonance of a single ZnO nanobelt, induced by an alternative electric field, was studied by *in situ* transmission electron microscopy (TEM). Due to the rectangular cross section of the nanobelt, two fundamental resonance modes have been observed corresponding to the two orthogonal transverse vibration directions. The mechanical resonant behavior of the nanobelts is directly correlated with their distinct structural feature, showing a possibility for versatile applications as nanoresonators and nanocantilevers.

Recently, an experimental approach, based on the electric-field-induced resonant excitation, has been developed for directly measuring the mechanical properties of individual nanowirelike structures by *in situ* TEM.[14,15] Using this method, the mechanical properties of carbon nanotubes,[14] silicon nanowires,[16] and silicon carbide–silica composite nanowires[17] have been investigated. This is the technique that will be applied to study the resonance behavior of individual ZnO nanobelts.

Scanning electron microscopy (SEM) image of the as-synthesized ZnO nanobelts is given in Fig. 1(a), which reveals a large quantity of nanobelts with lengths over several tens to hundreds of micrometers. Figure 1(b) shows a typical TEM image of the ZnO nanobelt, displaying high structural uniformity. The selected area electron diffraction pattern indicates that the nanobelt grows along [0001] and is enclosed by $\pm(2\bar{1}\bar{1}0)$ and $\pm(01\bar{1}0)$ facets.[6] Figure 1(c) represents the geometry of a nanobelt with length L, width W, and thickness T. In our experiment, the nanobelts were glued at one end onto a copper wire, while the other end near the counterelectrode was free. This is a simple one-end clamped cantilever with a rectangular cross section.

To carry out the mechanical property measurements of a nanobelt, a specimen holder for a Hitachi HF-2000 TEM (200 kV) was built for applying a voltage across a nanobelt and its counter electrode. The specimen holder has two electrodes and a set of piezomanipulation and translation devices. The nanobelts were attached to a solid gold ball of 0.1 mm in diameter and its counterelectrode is also a gold ball. An oscillating voltage with tunable frequency was applied across the two electrodes. Since the electric induced charge on the tip of the nanobelt oscillates at the frequency of the applied voltage, thus, mechanical resonance is induced if the applied frequency matches the natural vibration frequency

[a]Also at: International Center for Quantum Structures and State Key Laboratory for Surface Physics, Institute of Physics, Chinese Academy of Sciences, Beijing 100080, China.
[b]Author to whom correspondence should be addressed; electronic mail: zhong.wang@mse.gatech.edu

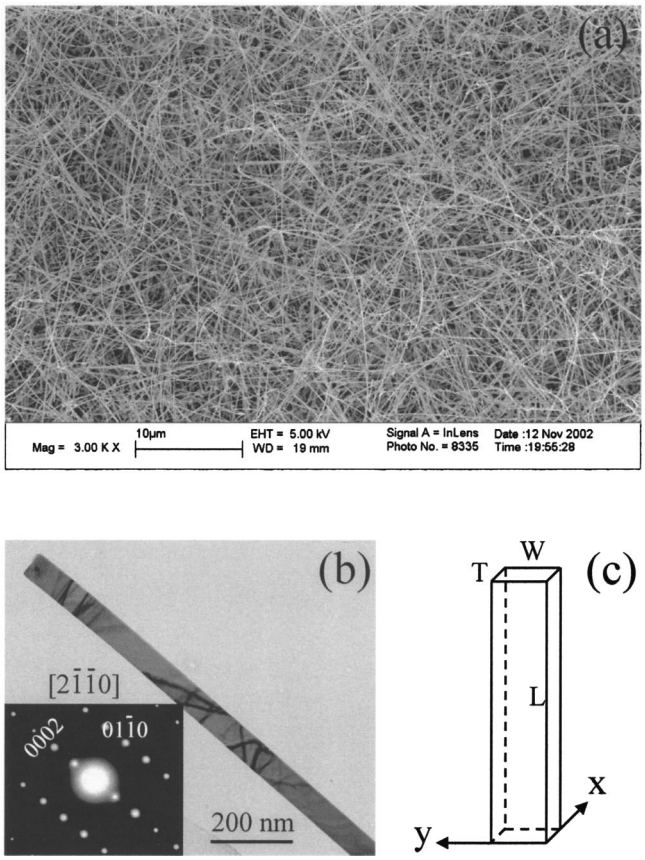

FIG. 1. (a) SEM image of the as-synthesized ZnO nanobelts. (b) A typical TEM image of a ZnO nanobelt and its electron diffraction pattern (inset). (c) Schematic geometrical shape of the nanobelt.

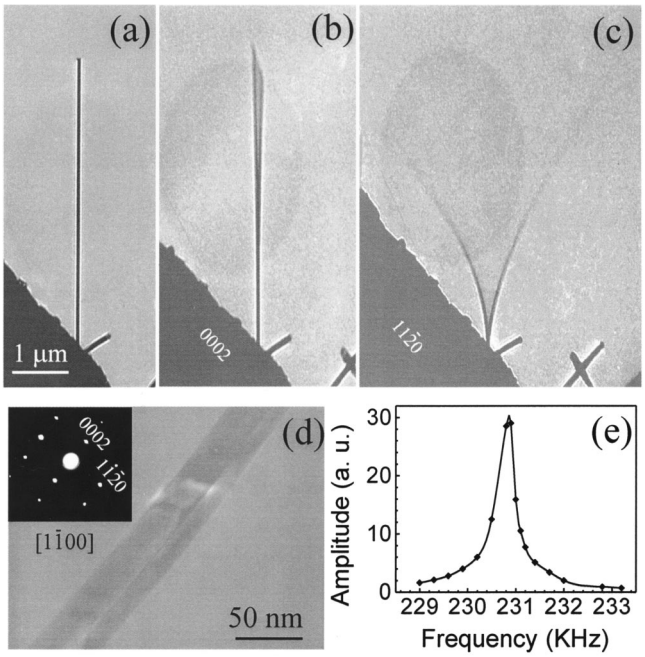

FIG. 2. A selected ZnO nanobelt at (a) stationary, (b) the first harmonic resonance in x direction, $\nu_{x1}=622$ kHz, and (c) the first-harmonic resonance in y direction, $\nu_{y1}=691$ kHz. (d) An enlarged image of the nanobelt and its electron diffraction pattern (inset). The projected shape of the nanobelt is apparent. (e) The FWHM of the resonance peak measured from another ZnO nanobelt. The resonance occurs at 230.9 kHz.

(Fig. 2). The resonance is directly viewed on the TV screen attached to the TEM. From the classical elasticity theory for a rectangular beam,[18] the fundamental resonance frequency corresponding to the thickness direction (x axis) [Fig. 1(c)] is

$$\nu_{xi}=\frac{\beta_i^2 T}{4\pi L^2}\sqrt{\frac{E_x}{3\rho}}, \tag{1}$$

where β_i is a constant for the ith harmonic: $\beta_1=1.875$ and $\beta_2=4.694$, E_x is the bending modulus for the vibration along the x axis, L is length of the nanobelt, ρ is mass density; and the corresponding resonance frequency in the width direction (y axis) [Fig. 1(c)] is given by

$$\nu_{yi}=\frac{\beta_i^2 W}{4\pi L^2}\sqrt{\frac{E_y}{3\rho}}. \tag{2}$$

The ratio of the two fundamental frequencies is directly related to the aspect ratio of the nanobelt by $\nu_{y1}/\nu_{x1}=W/T(E_y/E_x)^{1/2}$.

A stationary selected ZnO nanobelt is given in Fig. 2(a). By changing the frequency of the applied voltage, we have found two fundamental frequencies in two orthogonal transverse vibration directions. Figure 2(b) shows a harmonic resonance with its vibration plane nearly parallel to the viewing direction, and Fig. 2(c) shows the harmonic resonance with the vibration plane closely perpendicular to the viewing direction. For calculating the bending modulus, it is critical to accurately measure the fundamental resonance frequency (ν_1) and the dimensional sizes (L, W, and T) of the investigated ZnO nanobelts. To determine ν_1, we have checked the stability of resonance frequency to ensure one end of the nanobelt is tightly fixed, and the resonant excitation has been carefully checked around the half value of the observed resonance frequency to ensure it is the fundamental frequency. The specimen holder is rotated about its axis so that the nanobelt is aligned perpendicular to the electron beam, thus, the real length (L) of the nanobelt can be obtained. The normal direction of the wide facet of the nanobelt could be first determined by an electron diffraction pattern, which was [$2\bar{1}\bar{1}0$] for the ZnO nanobelt [Fig. 1(b)]. Then, the nanobelt was tilted from its normal direction by rotating the specimen holder, and the tilting direction and angle were determined by the corresponding electron diffraction pattern. As shown in the inset of Fig. 2(d), the electron-beam direction is [$1\bar{1}00$]. The angle between [$1\bar{1}00$] and [$2\bar{1}\bar{1}0$] is 30°, i.e., the normal direction of the wide facet of this nanobelt is 30° tilted from the direction of the electron beam. Using the projected dimension measured from the TEM image [Fig. 2(d)], the geometrical parameters of this nanobelt are determined to be $W=28$ nm and $T=19$ nm. Based on the experimentally measured data, the bending modulus of the ZnO nanobelts is calculated using Eqs. (1) and (2). The experimental results are summarized in Table I. The bending modulus of the ZnO nanobelts was ~52 GPa. This value represents the modulus that includes the scaling effect and geometrical shape, and it cannot be directly compared to the Young's modulus of ZnO ($c_{33}=210$ GPa and $c_{13}=104$ GPa),[19] because the shape of the nanobelt and the anisotropic structure of ZnO are convoluted in the measurement. The bending modulus measured by the resonance technique has excellent agreement with the elastic modulus measured by a nanoindenter for the same type of nanobelts.[20] Although nanobelts of different sizes

TABLE I. Bending modulus of the ZnO nanobelts. E_x and E_y represent the bending modulus corresponding to the resonance along the thickness and width directions, respectively.

Nanobelt	Length L (μm) (± 0.05)	Width W (nm) (± 1)	Thickness T (nm) (± 1)	Fundamental frequency (kHz)				Bending modulus (GPa)	
				W/T	ν_{x1}	ν_{y1}	ν_{y1}/ν_{x1}	E_x	E_y
1	8.25	55	33	1.7	232	373	1.6	46.6 ± 0.6	50.1 ± 0.6
2	4.73	28	19	1.5	396	576	1.4	44.3 ± 1.3	45.5 ± 2.9
3	4.07	31	20	1.6	662	958	1.4	56.3 ± 0.9	64.6 ± 2.3
4	8.90	44	39	1.1	210	231	1.1	37.9 ± 0.6	39.9 ± 1.2

may have a slight difference in the bending modulus, there is no obvious difference if the calculation were done using either Eqs. (1) or (2). The ratio of two fundamental frequencies ν_{y1}/ν_{x1} is consistent with the aspect ratio W/T, as expected from Eqs. (1) and (2), because there is no significant difference between E_x and E_y. The full width at half maximum (FWHM) of the resonance peak is shown in Fig. 2(e), and $\Delta\nu/\nu_1 \sim 0.2\%$ for a vacuum of 5×10^{-8} Torr, corresponding to a Q factor of ~ 500.

ZnO nanobelts can be used as a force sensor. Figure 3(a) shows a selected ZnO nanobelt with a hooked end, which is equivalent to a cantilever with an integrated tip. Due to the two transverse vibration modes of the nanobelt, resonance along two orthogonal directions has been observed [Figs. 3(b) and Fig. 3(c)]. The two resonance modes just correspond to the two modes of the tip operation when the nanobelt-based cantilever is used as a force sensor: One is the tapping mode, and the other is the noncontact mode. Thus, the force sensor fabricated using the ZnO nanobelts is versatile for applications on hard and soft surfaces.

In summary, mechanical resonance behavior of ZnO nanobelts has been characterized by *in situ* TEM. The bending modulus of the ZnO nanobelts is ~ 52 GPa and the damping time constant of nanobelt resonance in a vacuum of 10^{-8} Torr is ~ 1.2 ms. The dual-resonance modes with two orthogonal directions have been observed. The single crystalline structurally controlled nanobelts could be used as a type of nanoresonator and nanocantilever with dual-operation modes, which could be useful in nanoelectromechanical systems and highly functional nanodevices. Similar to carbon nanotubes, the nanobelts could also be used as functional tips for scanning probe microscopy.[21,22]

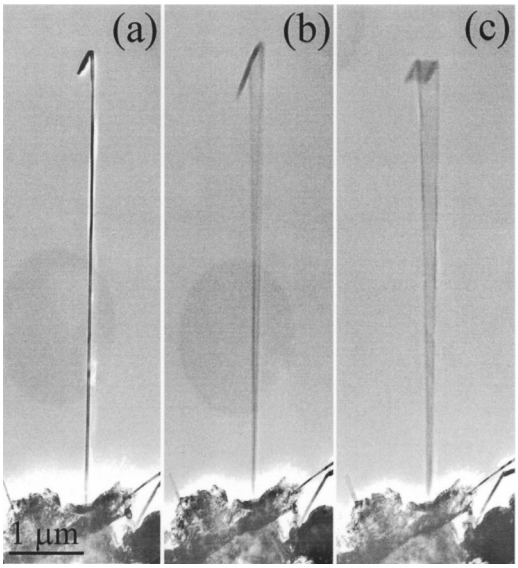

FIG. 3. A selected ZnO nanobelt with a hooked end at (a) stationary, (b) resonance at 731 kHz in the plane almost parallel to the viewing direction, and (c) resonance at 474 kHz in the plane closely perpendicular to the viewing direction.

The authors acknowledge support from the NASA URETI program (E-16-V14), China NSF, International Center for Quantum Structures (CAS), and Georgia Tech.

[1] R. Berger, C. Gerber, H. P. Lang, and J. K. Gimzewshi, Microelectron. Eng. **35**, 373 (1997).
[2] G. H. Wu, R. H. Datar, K. M. Hansen, T. Thundat, R. J. Cote, and A. Majumdar, Nature Biotechnology **19**, 856 (2001).
[3] K. A. Stevenson, A. Mehta, P. Sachenko, K. M. Hansen, and T. Thundat, Langmuir **18**, 8732 (2002).
[4] G. Abadal, Z. J. Davis, B. Helbo, X. Borrise, R. Ruiz, A. Boisen, F. Campabadal, J. Esteve, E. Figueras, F. Perez-Murano, and F. Barniol, Nanotechnology **12**, 100 (2001).
[5] Z. J. Davis, G. Abadal, O. Khn, O. Hansen, F. Grey, and A. Boisen, J. Vac. Sci. Technol. B **18**, 612 (2000).
[6] Z. W. Pan, Z. R. Dai, and Z. L. Wang, Science **291**, 1947 (2001).
[7] M. H. Huang, S. Mao, H. Feick, H. Yan, Y. Wu, H. Kind, E. Weber, R. Russo, and P. Yang, Science **292**, 1897 (2001).
[8] M. S. Arnold, P. Avouris, Z. W. Pan, and Z. L. Wang, J. Phys. Chem. B (to be published).
[9] E. Comini, G. Faglia, G. Sberveglieri, Z. Pan, and Z. L. Wang, Appl. Phys. Lett. **81**, 1869 (2002).
[10] Y. Cui, Q. Wei, H. Park, and C. M. Lieber, Science **293**, 1289 (2001).
[11] M. K. Gudiksen, L. J. Lauhon, J. Wang, D. C. Smith, and C. M. Lieber, Nature (London) **415**, 617 (2002).
[12] H. G. Craighead, Science **290**, 1532 (2000).
[13] W. Hughes and Z. L. Wang, Appl. Phys. Lett. (to be published).
[14] P. Poncharal, Z. L. Wang, D. Ugarte, and W. A. de Heer, Science **283**, 1513 (1999).
[15] Z. L. Wang, P. Poncharal, and W. A. de Heer, Pure Appl. Chem. **72**, 209 (2000).
[16] Z. L. Wang, Adv. Mater. (Weinheim, Ger.) **12**, 1295 (2000).
[17] Z. L. Wang, Z. R. Dai, Z. G. Bai, R. P. Gao, and J. Gole, Appl. Phys. Lett. **77**, 3349 (2000).
[18] L. Meirovich, *Elements of Vibration Analysis* (McGraw–Hill, New York, 1986).
[19] G. Carlotti, G. Socino, A. Petri, and E. Verona, Appl. Phys. Lett. **51**, 1889 (1987).
[20] S. X. Mao, M. Zhao, and Z. L. Wang (unpublished).
[21] H. J. Dai, J. H. Hafner, A. G. Rinzler, D. T. Colbert, and R. E. Smalley, Nature (London) **384**, 147 (1996).
[22] S. S. Wong, E. Joselevich, A. T. Woolley, C. L. Cheung, and C. M. Lieber, Nature (London) **394**, 52 (1998).